Electronic Supplementary Material (ESI) for Journal of Materials Chemistry A.
This journal is © The Royal Society of Chemistry 2019

Supporting Information

Uniform Li deposition by regulating initial nucleation barrier via simple liquid metal coating for dendrite-free Li metal anode

Chuanliang Wei,[a] Huifang Fei,[a] Yongling An,[a] Yuan Tao,[a] Jinkui Feng*[a] and Yitai Qian[b]

[a.]SDU & Rice Joint Center for Carbon Nanomaterials, Key Laboratory for Liquid–Solid Structural Evolution & Processing of Materials (Ministry of Education), School of Materials Science and Engineering, Shandong University, Jinan 250061, China. Email：jinkui@sdu.edu.cn

[b.]Hefei National Laboratory for Physical Science at Microscale, Department of Chemistry, University of Science and Technology of China, Hefei 230026, P. R. China

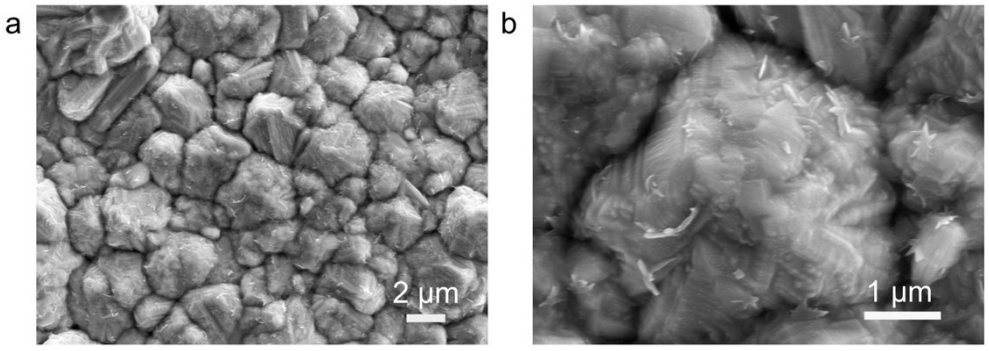

Fig. S1 (a, b) SEM images of CF.

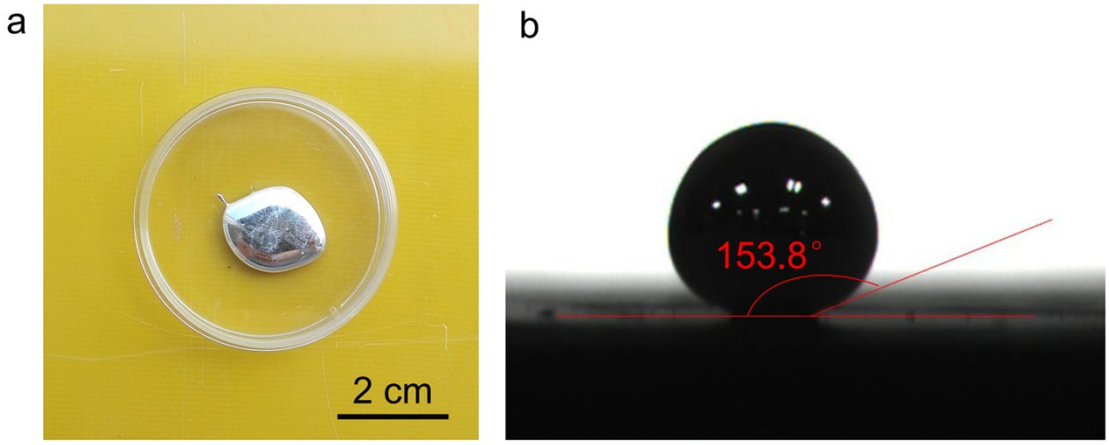

Fig. S2 (a) Optical image of 3℃ GaInSnZn liquid metal. (b) The contact angle of liquid metal on CF by dropping 4 μL liquid metal.

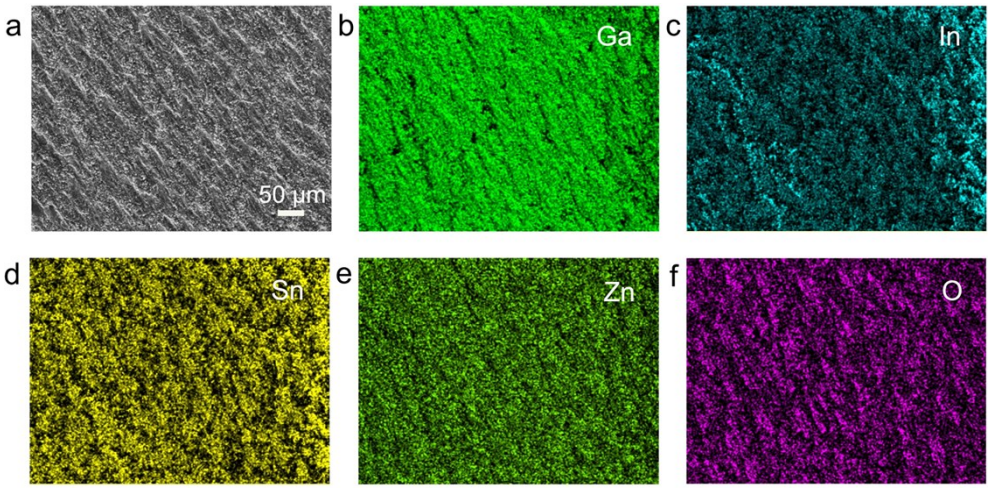

Fig. S3 (a) SEM image of LCF. (b–f) Corresponding EDS elemental mapping of Ga, In, Sn, Zn and O, respectively.

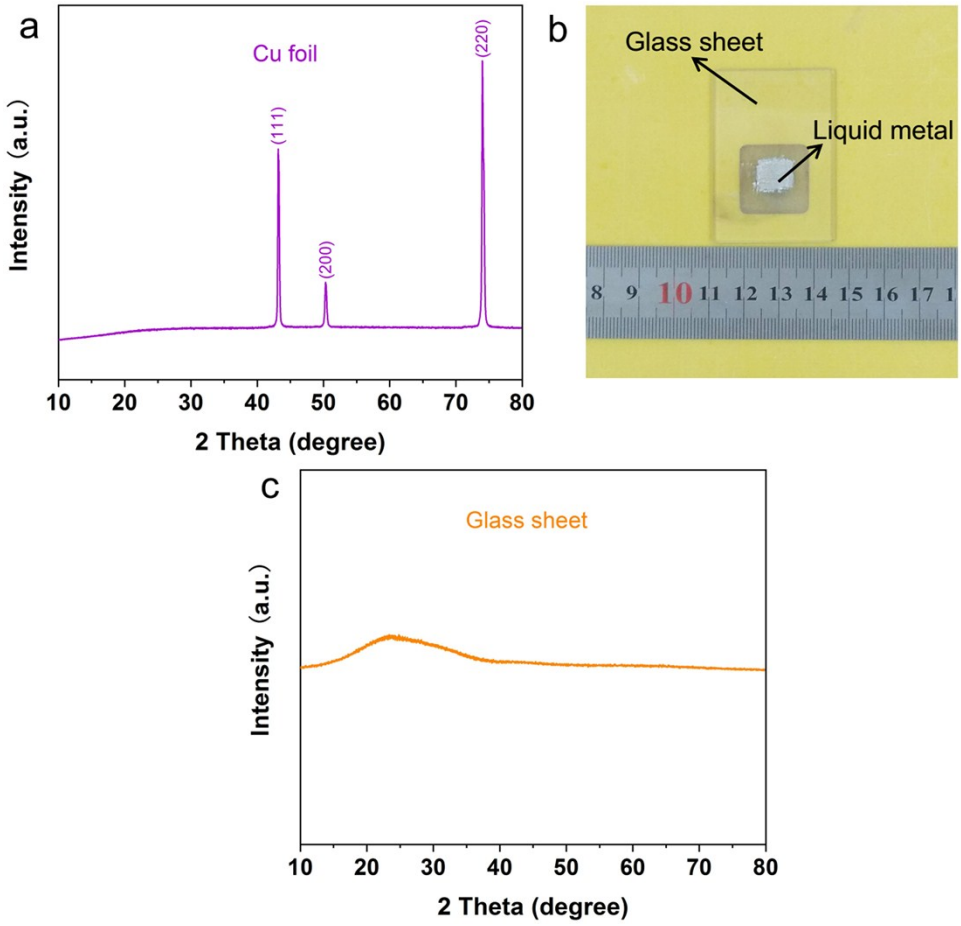

Fig. S4 (a) XRD patterns of CF. (b) Glass sheet coated with a liquid metal layer using a small brush for XRD test. (c) XRD patterns of the glass sheet.

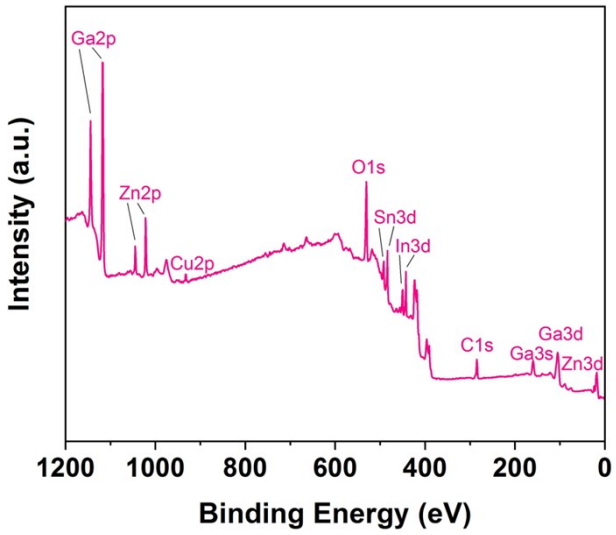

Fig. S5 XPS full spectrum of LCF.

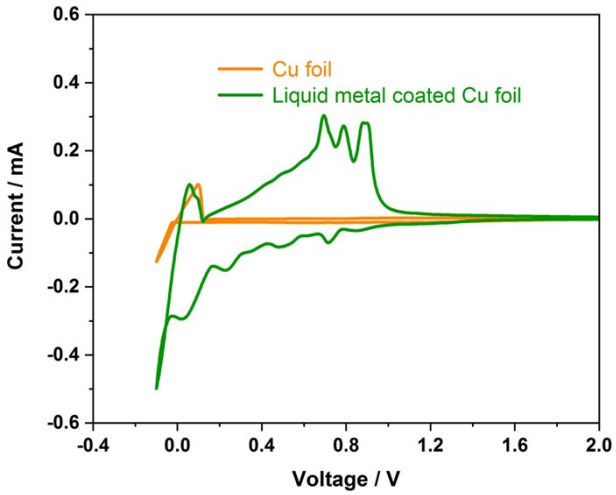

Fig. S6 CV curves of CF and LCF in -0.1–2.0 V with a scan rate of 0.05 mV s^{-1}.

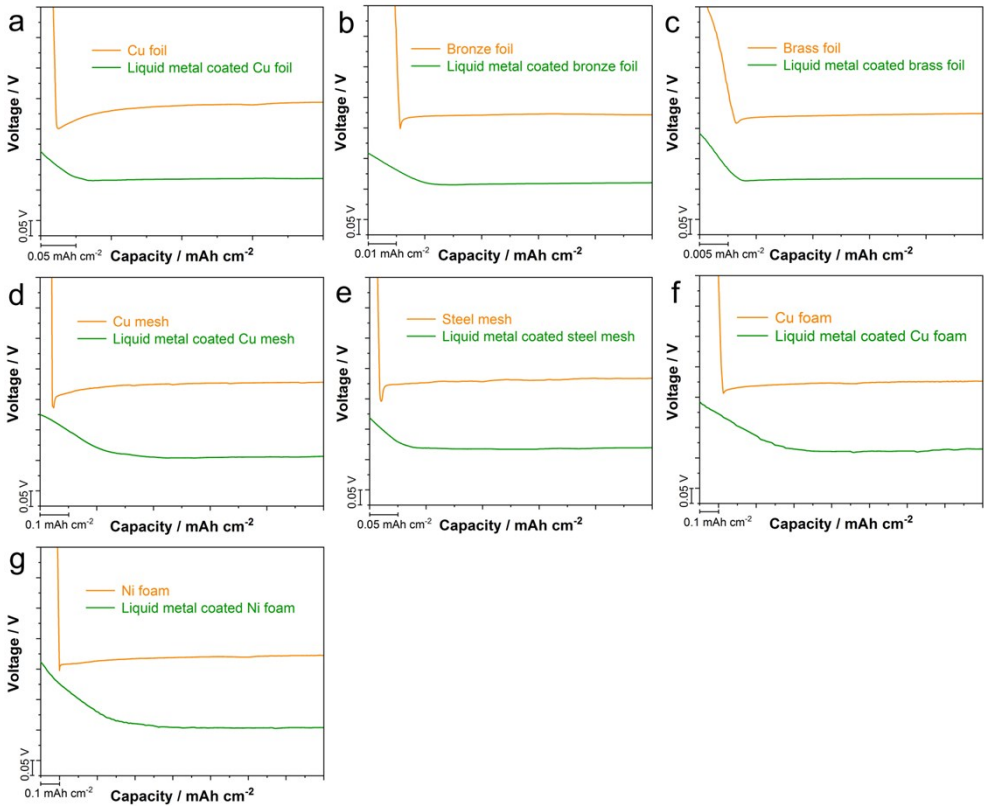

Fig. S7 Voltage-capacity curves of various current collectors before and after liquid metal coating at 0.2 mA cm^{-2}. For comparison, the curves are shifted horizontally or vertically based on the onset of lithium nucleation.

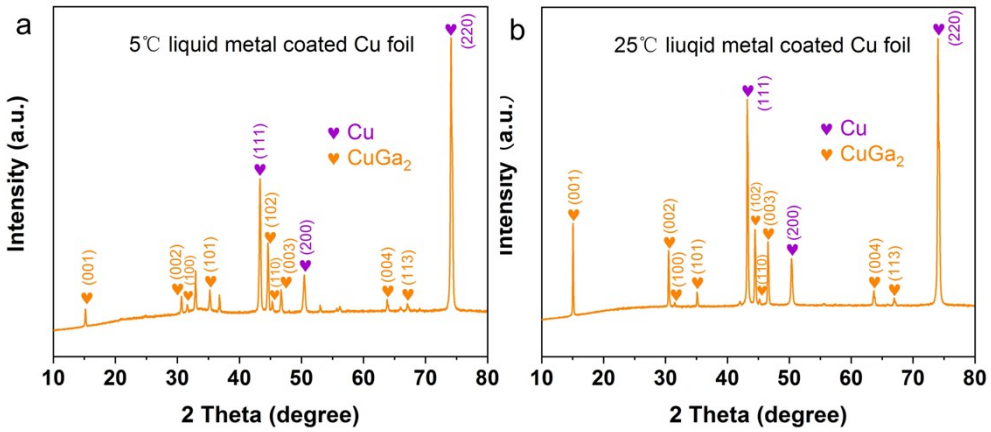

Fig. S8 (a, b) XRD patterns of 5 ℃ and 25 ℃ liquid metal coated Cu foil, respectively.

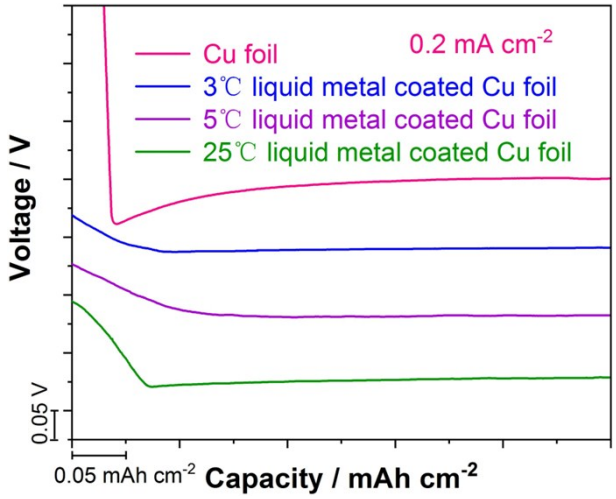

Fig. S9 Voltage-capacity curves of CF and CF with 3, 5 and 25 ℃ liquid metal coating at 0.2 mA cm^{-2}. For comparison, the curves are shifted horizontally or vertically based on the onset of lithium nucleation.

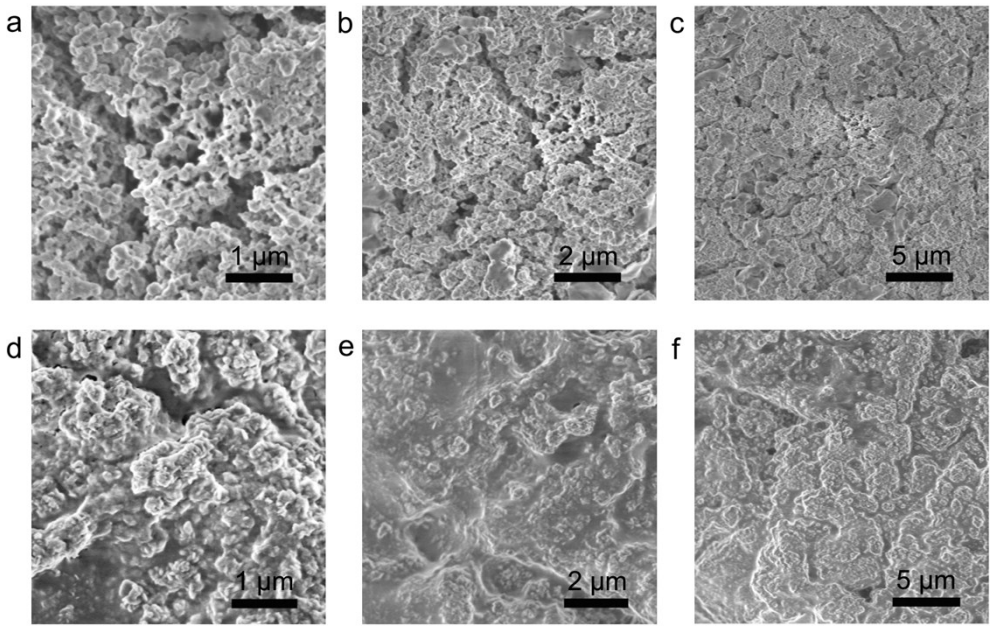

Fig. S10 (a–c) SEM images of CF after depositing 1.0 mAh cm^{-2} of Li. (d–f) SEM images of LCF after depositing 1.0 mAh cm^{-2} of Li.

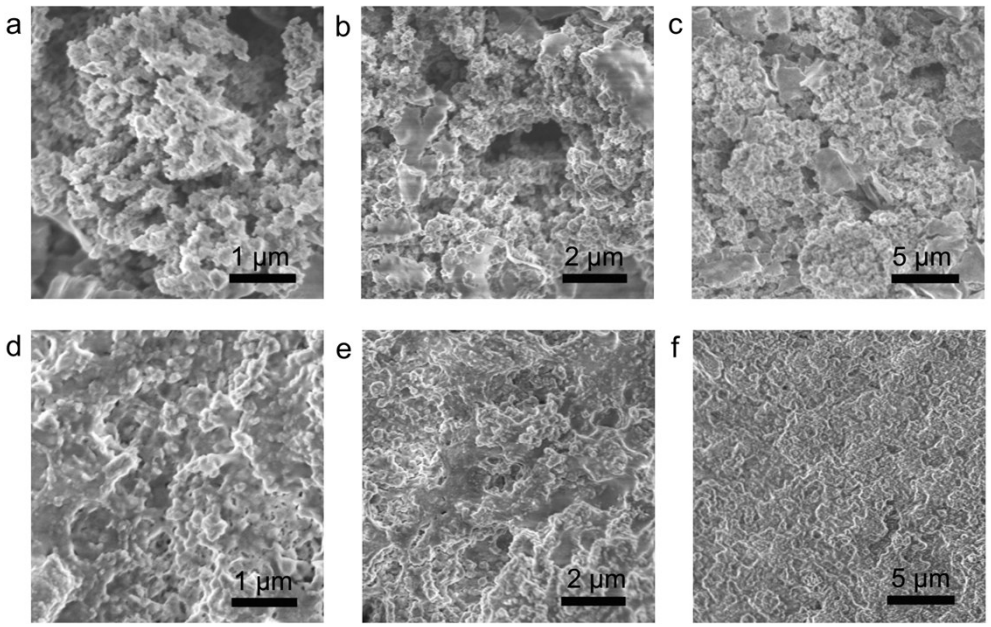

Fig. S11 (a–c) SEM images of CF after depositing 2.0 mAh cm^{-2} of Li. (d–f) SEM images of LCF after depositing 2.0 mAh cm^{-2} of Li.

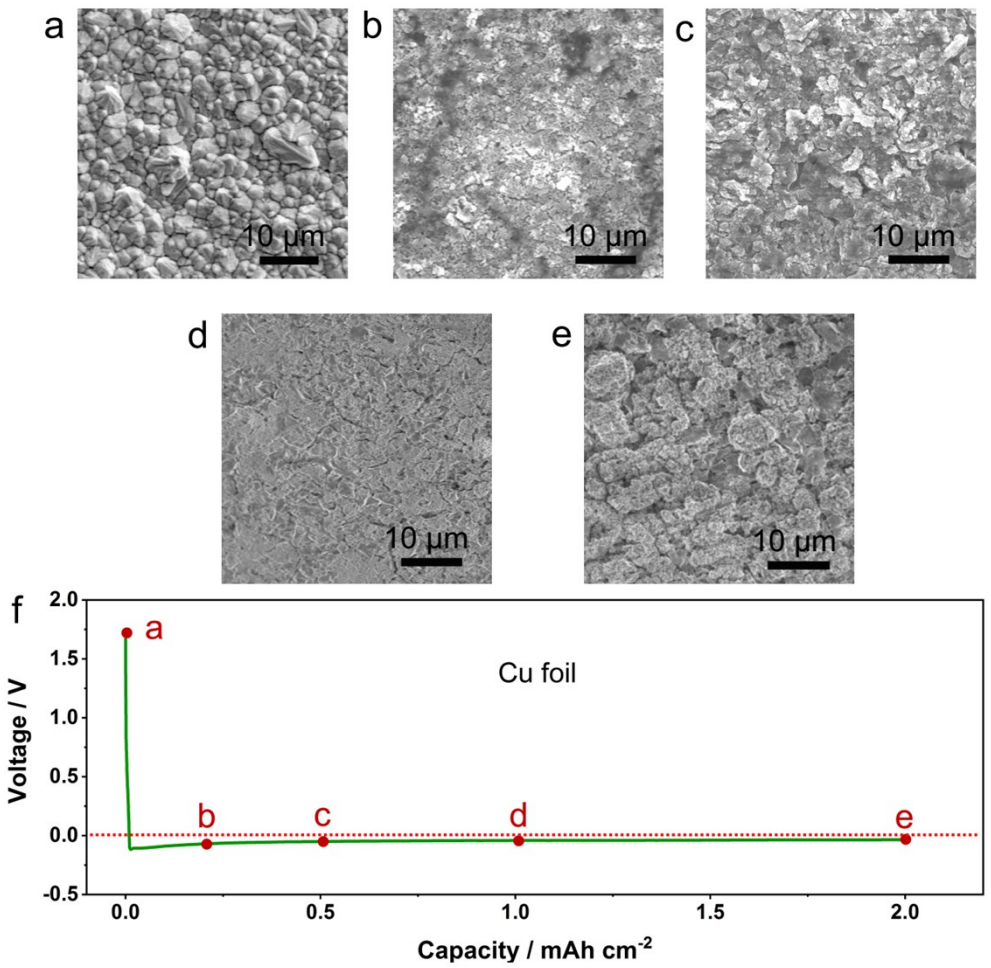

Fig. S12 (a) SEM images of CF. (b–e) SEM images of LCF when depositing 0.2, 0.5, 1.0 and 2.0 mAh cm^{-2} of Li, respectively. (f) Discharge curve of CF at a current density of 0.2 mA cm^{-2} with a total Li deposition of 2.0 mAh cm^{-2}.

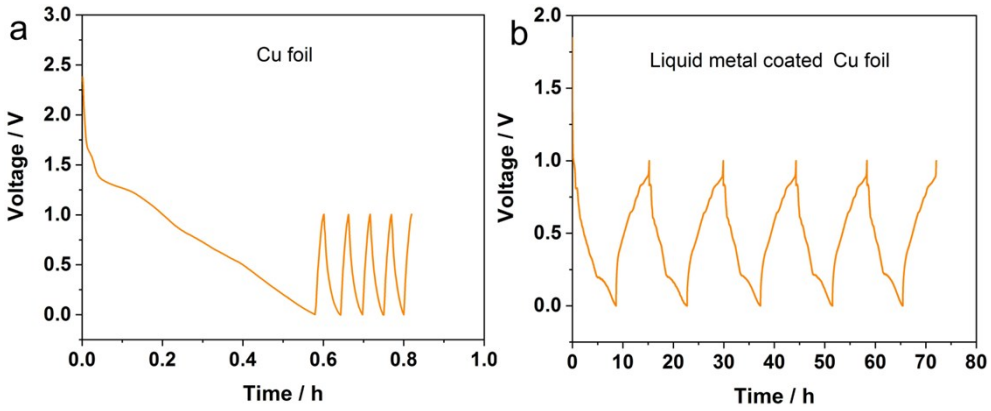

Fig. S13 (a, b) Charge-discharge curves of CF and LCF in 0–1.0 V at 50 μA, respectively.

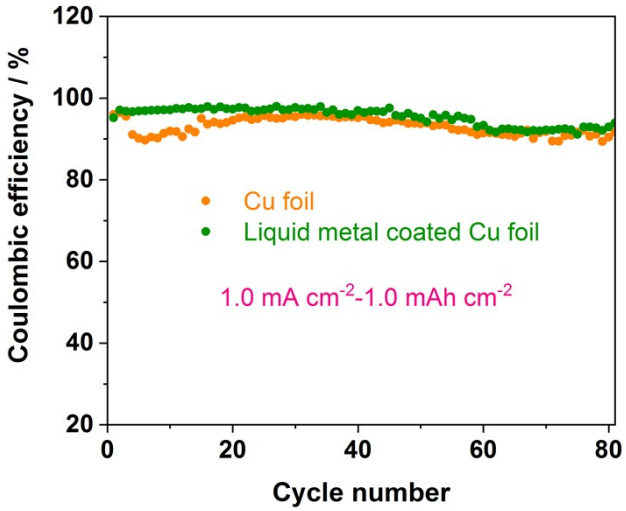

Fig. S14 The Coulombic efficiency of CF and LCF at 1.0 mA cm^{-2} with Li deposition of 1.0 mAh cm^{-2}.

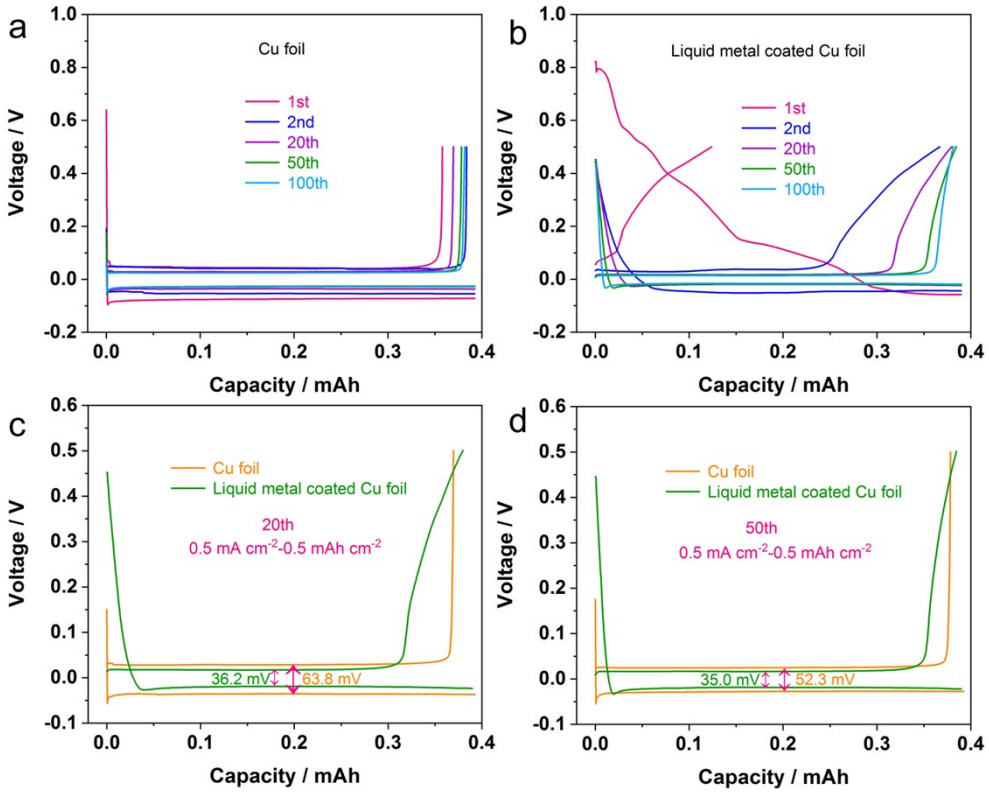

Fig. S15 (a, b) Charge-discharge curves of CF and LCF at 0.5 mA cm^{-2} with Li deposition of 0.5 mAh cm^{-2}, respectively. (c) The 20th charge-discharge curves of CF and LCF at 0.5 mA cm^{-2} with Li deposition of 0.5 mAh cm^{-2}. (d) The 50th charge-discharge curves of CF and LCF at 0.5 mA cm^{-2} with Li deposition of 0.5 mAh cm^{-2}.

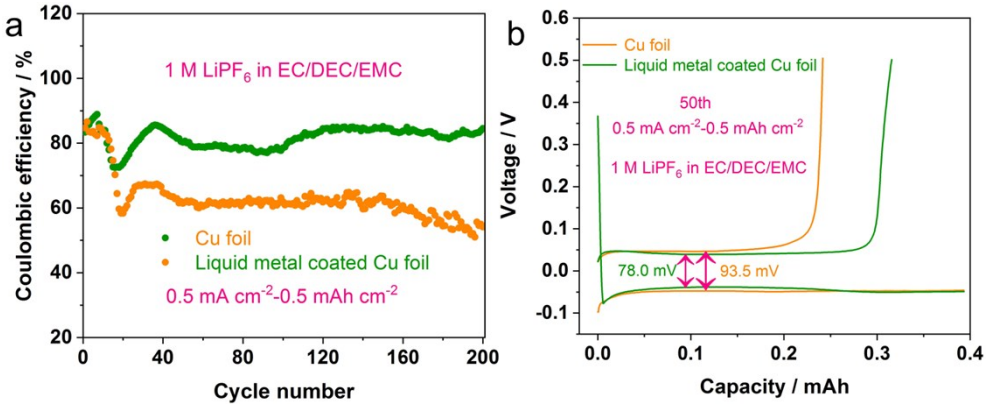

Fig. S16 (a) The Coulombic efficiency of CF and LCF in carbonate electrolyte at 0.5 mA cm^{-2} with Li deposition of 0.5 mAh cm^{-2}. (b) The 50th charge-discharge curves of CF and LCF at 0.5 mA cm^{-2} with Li deposition of 0.5 mAh cm^{-2}.

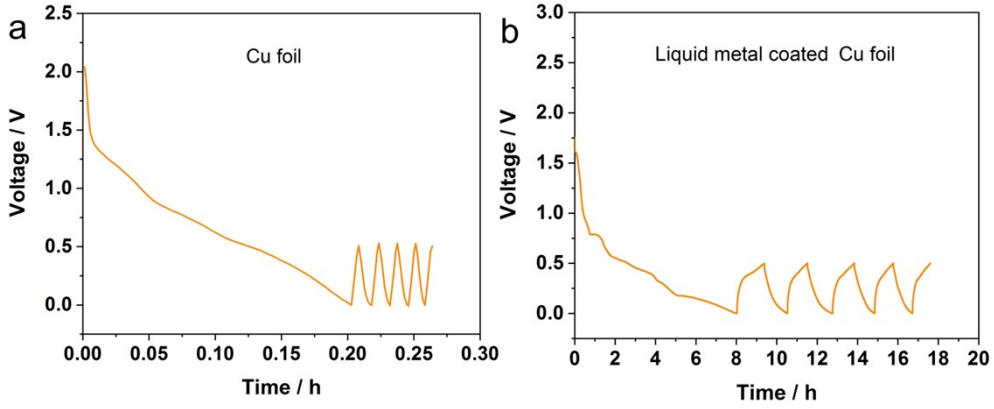

Fig. S17 (a, b) Charge-discharge curves of CF and LCF in 0–0.5 V at 50 μA, respectively.

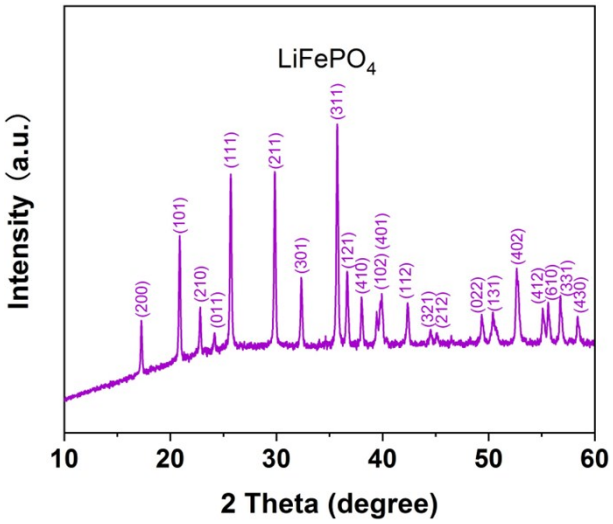

Fig. S18 XRD patterns of $LiFePO_4$ cathode materials.

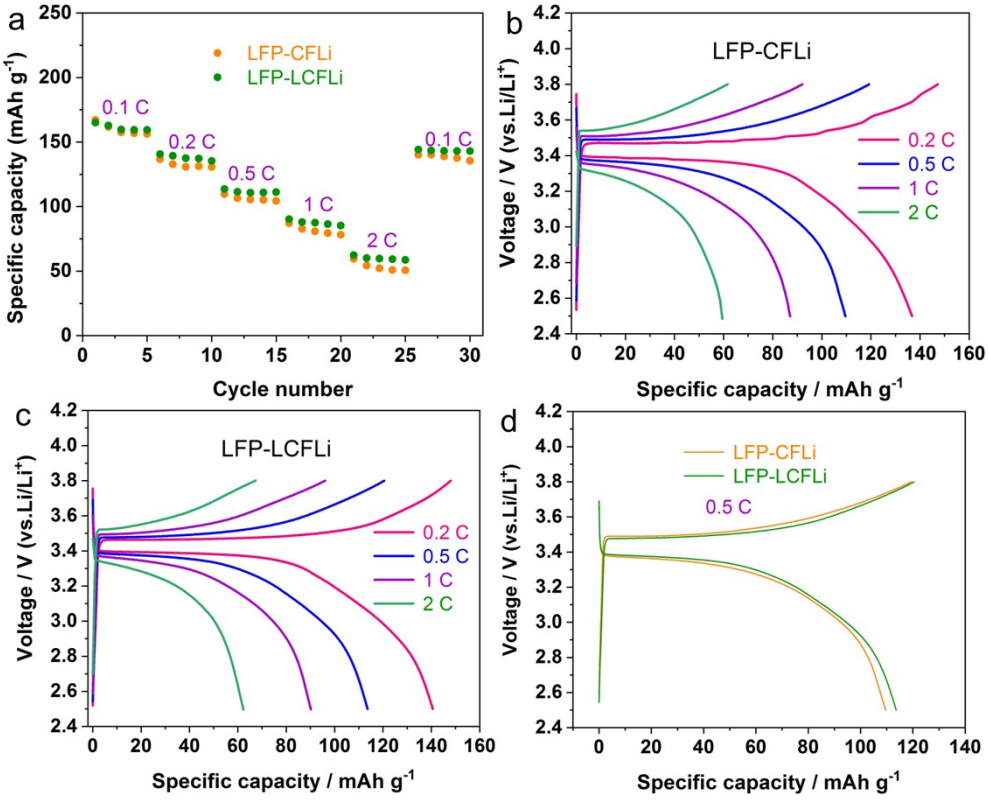

Fig. S19 (a) Rate capabilities of LFP-CFLi and LFP-LCFLi full cells. (b, c) Charge-discharge curves of LFP-CFLi and LFP-LCFLi at different rates, respectively. (d) Charge-discharge curves of LFP-CFLi and LFP-LCFLi at 0.5 C.

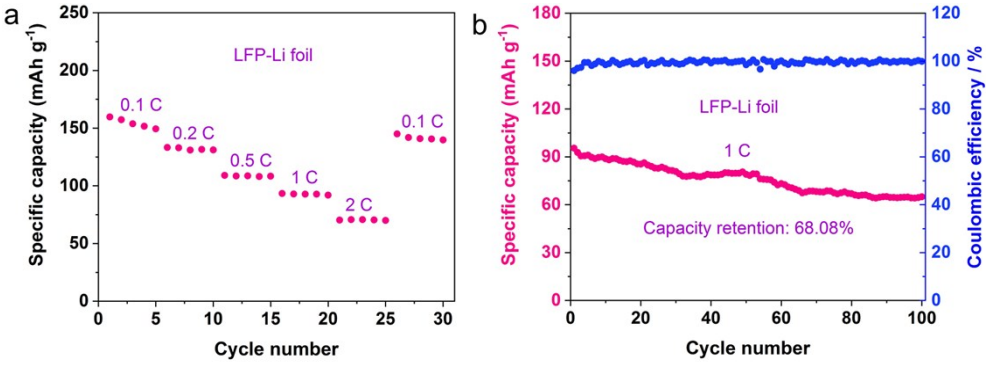

Fig. S20 (a) Rate capability of LFP-Li foil half cells. (b) Cycling performance of LFP-Li foil half cells at 1 C.